

NUMERICAL SIMULATION OF VISCOELASTIC FLOWS IN A FLAT SLIT CHANNEL

Yong Li, Jianrong Zheng and Xinling Ma

ABSTRACT

The slit channel flow is a typical problem in the dies of plastic films and sheets. The mathematical model of three-dimensional viscoelastic fluids flow in the slit channel of the sheets dies is established. A new finite element method named the finite piece method is proposed to simulated planar slit flow with K-BKZ integral constitutive model. According to this method the velocity distributions in thickness direction is approach by Fourier series. Then the three dimensional finite element equations can be simplified to two dimensional. Picard iteration method is used to solve nonlinear equation. The extra-stress tensor is calculated by integrating along path line. The new method has been tested in channel with constant thickness and variable thickness. The results of the simulation are compared to three-dimensional simulation using the finite element method. This comparison shows that the distributions of velocity and the pressure obtained by simulation agree well with those of 3D FEM. The new methods proposed in the study can be well used to predict slit flow of viscoelastic fluids.

Keywords: viscoelastic fluid; slit channel; the finite piece method; numerical simulation

1. INTRODUCTION

Extrusion molding is one of the most important fields of plastic manufacturing while the extrusion die is crucial for the success of the extrusion molding process. In order to produce excellent plastic product with the extrusion die, we must consider the optimization of the flow channel.

Flow behavior of polymeric liquids in polymer processing affects both the quality of products and process efficiency. Polymeric melt is viscoelastic and its flow behavior is generally more complex than their Newtonian counterparts. Hence, viscoelastic flows have been studied both experimentally and numerically using various model channels that have characteristic geometries such as contraction, expansion, slit, and cavity. In polymer processing the flow is essentially three-dimensional. Therefore, it becomes important to understand three-dimensional flow behavior of polymeric liquids. Meanwhile in the case of predicting the polymer processing by computer aided engineering, one constitutive equation which can accurately describe experimental melt theology under shear, uniaxial, biaxial, and planar deformations is indispensable. With such background, several constitutive equations have been proposed and evaluated. In the past differential constitutive equation are often used to deal with three-dimensional flow [1~6].

However because of its wide applicability, the K-BKZ integral equation has been extensively examined. Previous studies have shown that the K-BKZ model is able to describe uniaxial, biaxia and planar elongation viscosity [7, 8]. In general, integral constitutive models of the K-BKZ type have performed well in prediction of isothermal polymer behavior in complex flow situations. This was initiated with the simulation of two-dimensional steady contraction flow [9~11] and extrusion flow of the IUPAC-LDPE melt [12, 13, 18]. More recent studies consider three-dimensional flow and time dependent flow [14~17] which quantitative agreement between experiments and simulations was observed generally.

The manufacture of plastic films and sheets is frequently accomplished by using the coat-hanger dies and fishtail dies. Thickness of the channel is very small and the length and width is very large. The slit flow is a typical

* School of Mechanical and Power Engineering, East China University of Science and Technology, Shanghai, 200237, China, E-mail: yong_li@ecust.edu.cn

problem in this kind of dies. For last several years, many numerical methods have been adopted for the prediction of complex flow, including the finite difference method (FDM), the finite element method (FEM) and the finite volume method (FVM). Traditional finite element method can deal with flow problem of three-dimensional polymer melt in these dies, but an exact mathematical analysis of viscoelastic flow in the die is a very challenging proposition because of the complexities with geometrical and viscoelastic effects. For the slit flow, the thickness is very thinner than length and width, and our main concern is the velocity distribution along the width direction, so a complete three-dimensional analysis is often wasteful and unnecessary. Especially in the computer-aided design, we always want to build another way to reduce the workload by making pre-treatment more convenient and saving memory and CPU time.

In solid mechanics finite element structural analysis, there is a special three-dimensional structure which is both the geometry and material properties do not change along a certain coordinate, but load and displacement are changeable. So we can not deal with the problem as a two-dimensional plane strain, generally, it is analyzing as a three-dimensional problem by the finite element method. Y. K. Cheung proposes the finite strip method [19] to deal with the problem. It is to use the series satisfying the boundary conditions to approach the displacement in some direction. This method has been widely applied and developed in solid mechanics.

It is the inspiration from application of the finite strip method in solid mechanics, the finite piece method (FPM) is established to predict viscoelastic flow through a planar slit channel in this paper. It is a finite element semi-analytical method which can be adopted to reduce the computation memory requirement for three dimensional problems. It is different from the finite strip method, its element is flat, but the element of the finite strip method is slender. Since the K-BKZ integral constitutive equation has shown much excellence in other viscoelastic simulation, we use such constitutive equation to describe the flow of polymer melts in channel. The results are compared with those calculated by 3D finite element method.

The paper is organized as follows. In Section 2, we present the system of governing equations that are used in the simulations. Next in Section 3, we describe in more detail the solution of the finite piece method adopted in the calculations. Finally, we compare the distributions of velocity and pressure in the planar flow channel, respectively, obtained by the finite piece method and 3D FEM in Section 4.

2. GOVERNING EQUATIONS

The flow is governed by the general equations for mass and momentum. Considering the characteristics of the polymer melts flow in a die channel, for an incompressible fluid under iso-thermal, creeping flow conditions ($Re=0$), the continuity equation and the motion equation are given by

$$\nabla \cdot \mathbf{V} = 0, \quad (1)$$

$$-\nabla P + \nabla \cdot \boldsymbol{\tau} = 0 \quad (2)$$

where \mathbf{V} is the velocity vector, $\boldsymbol{\tau}$ is the extra-stress tensor, and P is the scalar pressure. The constitutive equation that relates $\boldsymbol{\tau}$ to the deformation history is an integral K-BKZ equation where the extra stress tensor is calculated according to the modified PSM model [12] and can be expressed in its general form as follows

$$\boldsymbol{\tau}(t) = \frac{1}{1-\theta} \int_{-\infty}^t \sum_{k=1}^N \frac{a_i}{\lambda_i} \exp\left(-\frac{t-t'}{\lambda_i}\right) \frac{\alpha}{(\alpha-3) + \beta_i I_{C^{-1}} + (1-\beta_i) I_C} [C^{-1} + \theta C] dt', \quad (3)$$

where λ_i and a_i are the relaxation times and relaxation modulus coefficients respectively at a reference temperature, α and β_i are material constants, $I_{C^{-1}}$, I_C are the first invariants of the Cauchy-Green tensor C and the Finger strain tensor C^{-1} , θ is the material constant given by

$$\frac{N_2}{N_1} = \frac{\theta}{1-\theta}, \quad (4)$$

where N_1 and N_2 are the first and second normal stress differences, respectively.

For slit flow, the size of thickness is much less than others. We create Cartesian coordinate system which the z axis is the thickness direction of slit channel, as shown in Fig. 1, so the continuity equation is

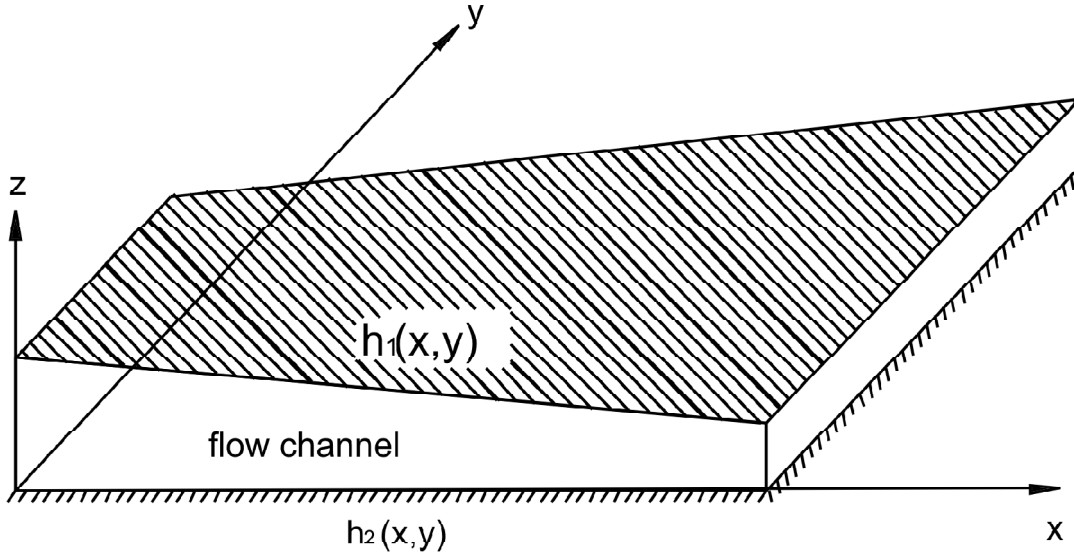


Figure 1: Schematic Diagram of the Slit Channel Geometry and Coordinate System

$$\frac{\partial v_x}{\partial x} + \frac{\partial v_y}{\partial y} + \frac{\partial v_z}{\partial z} = 0. \quad (5)$$

If the lower surface of the channel is $h_1(x, y)$, the upper surfaces is $h_2(x, y)$, let us integral along the thickness

$$\int_{h_1}^{h_2} \frac{\partial v_x}{\partial x} dz + \int_{h_1}^{h_2} \frac{\partial v_y}{\partial y} dz + \int_{h_1}^{h_2} \frac{\partial v_z}{\partial z} dz = 0, \quad (6)$$

and define the volumetric flow as follow

$$q_x = \int_{h_1}^{h_2} v_x dz, \quad (7)$$

$$q_y = \int_{h_1}^{h_2} v_y dz. \quad (8)$$

we obtain

$$\begin{aligned} & \frac{\partial q_x}{\partial x} + \frac{\partial q_y}{\partial y} \\ &= v_x(h_2) \frac{\partial h_2}{\partial x} + v_y(h_2) \frac{\partial h_2}{\partial y} - v_z(h_2) - [v_x(h_1) \frac{\partial h_1}{\partial x} + v_y(h_1) \frac{\partial h_1}{\partial y} - v_z(h_1)], \end{aligned} \quad (9)$$

It can be found that the right end item are the normal velocity of the upper and lower surface which are obviously zero, so the continuity equation about flow is

$$\frac{\partial q_x}{\partial x} + \frac{\partial q_y}{\partial y} = 0. \quad (10)$$

3. THE FINITE PIECE METHOD

The X, Y direction size of the slit channel is much longer than that of the thickness in Z direction; also, what we concern is the distribution of the flow in X, Y direction. So the key problem of the plates mold is to acquire the flow distributed in the X, Y direction. Because the flow is creeping and there is not secondary flow, e. q. vortex, the flow channel with varying thickness can be divided into several small parallel regions (element) of different height. The

flow inside the element can be assumed to be the same as those inside the parallel flow channel, and the velocity v_z can be ignored. But it remains to be a three-dimensional problem. Because the velocity and extra-stress are still the function of coordinate Z . We will make discrete element equations by the finite piece method which is a kind of finite element semi-analysis method, with flow and pressure as the unknown variables, and make the above-mentioned problem reduced to a similar two-dimensional problem to solve finally.

By the finite piece method, firstly, we assume the curves of the v_x, v_y in the Z direction in order that we can construct the finite element interpolating polynomial without the Z coordinate. As the Fourier series can approach any continuous functions given within the region, it is easy to approximate the curve by using the Fourier series. In other words, the finite piece method is to construct an approximation function of the velocity using finite element interpolating polynomial in some directions and using continuous smooth Fourier series meeting the boundary conditions in other directions. We postulate

$$v_x = \sum_{k=1}^R v_x^k(x, y) F_k(z) = \sum_{k=1}^R \sum_{i=1}^M \phi_i(x, y) v_{x_i}^k F_k(z) = \sum_{k=1}^R \sum_{i=1}^M \Phi_i^k v_{x_i}^k, \quad (11)$$

$$v_y = \sum_{k=1}^R v_y^k(x, y) F_k(z) = \sum_{k=1}^R \sum_{i=1}^M \phi_i(x, y) v_{y_i}^k F_k(z) = \sum_{k=1}^R \sum_{i=1}^M \Phi_i^k v_{y_i}^k, \quad (12)$$

the pressure approximation function still is

$$p = \sum_{i=1}^N \phi_i(x, y) p_i, \quad (13)$$

in the equations $v_{x_i}^k, v_{y_i}^k$ are nodal velocity corresponding to the k th item; p_i is node pressure. $\phi_i(x, y)$ is velocity shape function, $\varphi_i(x, y)$ is pressure shape function. $F_k(z)$ is the Fourier series which meet boundary conditions in the thickness direction. $\Phi_i^k = \phi_i(x, y) F_k(z) \cdot v_x^k(x, y), v_y^k(x, y)$ are interpolating function which are the multinomial with undetermined coefficient corresponding k th series item. R is the total number of the term taken in the series, M is total number of node with velocity, N is total number of node with pressure.

In the present paper, we use quadrilateral elements with a quadratic interpolation for the velocity and a linear interpolation for the pressure field. According to above ideas, we can only divide elements in the X - Y plane, but the 'elements' is the piece 11'22'33'44' with thickness of channel, as shown in Fig. 2, so we call this method the finite piece method. It is different from the finite strip method, its element is flat, and the element of the finite strip method is slender. For the finite elements method, the elements are connected by nodes but for the finite strip method they are connected by lines, e. g. 22', 33', 44' in Fig. 2. After constructing the velocity approximation function of X - Y plane, we can get the velocity distribution of the entire region according to Eqs. (11) and (12).

Applying Galerkin-weighted method to Eqs. (2) and (10), let residual value equal to Φ_i^k , φ_i and using Green-Gauss formula, we obtain

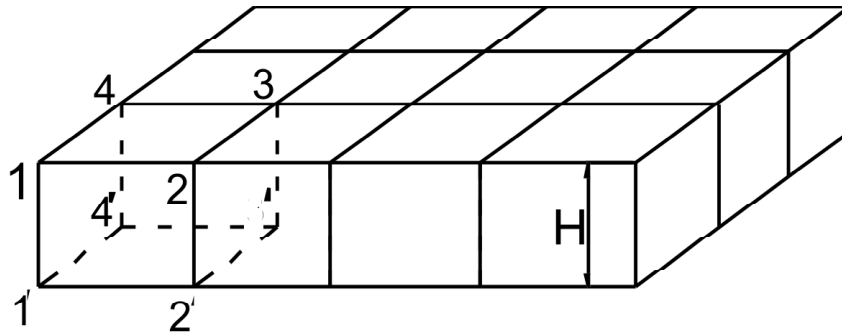


Figure 2: The Finite Piece Mesh with Thickness H

$$\int_{\Omega} (\nabla \Phi_i^k)^T \cdot (-p\mathbf{I} + \boldsymbol{\tau}) d\Omega = \int_{\Gamma} \mathbf{t} \Phi_i^k d\Gamma, \quad (14)$$

$$\int_{\Omega} \varphi_i \nabla \cdot \mathbf{q} d\Omega = 0, \quad (15)$$

where \mathbf{t} is the known surface force, \mathbf{q} is the volumetric flow.

As the constitutive equation is in the integral form, $\boldsymbol{\tau}$ is the integration of the function of strain tensor along the flow path, Eqs. (14) and (15) can not be converted into any explicit formulation of the unknown velocity. A very difficult problem with has not been solved as yet is the construction of Newton's procedure for calculating the velocity correction. So we use the Picard iteration method. Indeed, let $\mathbf{V}^{(n)}$, $\mathbf{q}^{(n)}$ and $p^{(n)}$ denote the values of velocity, flow, and pressure after n times' iteration, using below relation

$$\mathbf{V}^{(n+1)} = \mathbf{V}^{(n)} + \delta \mathbf{V}, \quad (16)$$

$$\mathbf{q}^{(n+1)} = \mathbf{q}^{(n)} + \delta \mathbf{q}, \quad (17)$$

$$p^{(n+1)} = p^{(n)} + \delta p, \quad (18)$$

the extra-stress tensor is calculated as follow

$$\boldsymbol{\tau}^{(n+1)} = \boldsymbol{\tau}^{(n)} + \eta(\nabla \delta \mathbf{V} + \nabla \delta \mathbf{V}^T), \quad (19)$$

is shear viscosity. So we obtain

$$\begin{aligned} & \int_{\Omega} (\nabla \Phi_i^k)^T \cdot [\delta p \mathbf{I} + \eta(\nabla \delta \mathbf{V} + \nabla \delta \mathbf{V}^T)] d\Omega, \\ & = - \int_{\Omega} (\nabla \Phi_i^k)^T \cdot [-p^{(n)} \mathbf{I} + \boldsymbol{\tau}^{(n)}] d\Omega + \int_{\Gamma} \mathbf{t} \Phi_i^k d\Gamma. \end{aligned} \quad (20)$$

$$\int_{\Omega} \varphi_i \nabla \cdot \delta \mathbf{q} d\Omega = \int_{\Omega} \varphi_i \nabla \cdot \mathbf{q}^{(n)} d\Omega \quad (21)$$

For the sheet slit channel, we assume that pressure is invariable along the thickness and it is only the function of x, y , so the third equation of the motive Eq. (2) can be simplified into

$$-\frac{\partial p}{\partial z} = 0, \quad (22)$$

and $v_z = 0$, the Eqs. (20) and (21) can be rewritten as the component type

$$\int_{\Omega} \left(-\delta P + 2\eta \frac{\partial \delta v_x}{\partial x} \right) \frac{\partial \Phi_i^k}{\partial x} d\Omega + \int_{\Omega} \eta \left(\frac{\partial \delta v_x}{\partial y} + \frac{\partial \delta v_y}{\partial x} \right) \frac{\partial \Phi_i^k}{\partial y} d\Omega + \int_{\Omega} \eta \frac{\partial \delta v_x}{\partial z} \frac{\partial \Phi_i^k}{\partial z} d\Omega \quad (23)$$

$$= - \int_{\Omega} \left(-P + \frac{\partial \tau_{xx}}{\partial x} \right) \frac{\partial \Phi_i^k}{\partial x} d\Omega - \int_{\Omega} \frac{\partial \tau_{yx}}{\partial y} \frac{\partial \Phi_i^k}{\partial y} d\Omega - \int_{\Omega} \frac{\partial \tau_{zx}}{\partial z} \frac{\partial \Phi_i^k}{\partial z} d\Omega + \int_{\Gamma} t_x \Phi_i^k d\Gamma$$

$$\int_{\Omega} \eta \left(\frac{\partial \delta v_y}{\partial x} + \frac{\partial \delta v_x}{\partial y} \right) \frac{\partial \Phi_i^k}{\partial x} d\Omega + \int_{\Omega} (-\delta P + 2\eta \frac{\partial \delta v_y}{\partial y}) \frac{\partial \Phi_i^k}{\partial y} d\Omega + \int_{\Omega} \eta \frac{\partial \delta v_y}{\partial z} \frac{\partial \Phi_i^k}{\partial z} d\Omega \quad (24)$$

$$= - \int_{\Omega} \frac{\partial \tau_{xy}}{\partial x} \frac{\partial \Phi_i^k}{\partial x} d\Omega - \int_{\Omega} \left(-P + \frac{\partial \tau_{yy}}{\partial y} \right) \frac{\partial \Phi_i^k}{\partial y} d\Omega - \int_{\Omega} \frac{\partial \tau_{zy}}{\partial z} \frac{\partial \Phi_i^k}{\partial z} d\Omega + \int_{\Gamma} t_y \Phi_i^k d\Gamma$$

$$\int_{\Omega} \left(\frac{\partial \delta q_x}{\partial x} + \frac{\partial \delta q_y}{\partial y} \right) \varphi_i d\Omega = \int_{\Omega} \left(\frac{\partial q_x}{\partial x} + \frac{\partial q_y}{\partial y} \right) \varphi_i d\Omega \quad (25)$$

Moreover, Eqs. (23) and (24) are available only inside the element. The velocity values of the same node in different element without same thickness are not equal; meanwhile, the flow values are continuous. So we convert the Eqs. (23) and (24) into equations with flow as the unknown variables so as to combine the element equations into global equation.

In the present paper, we only use the first item of series, so the velocity is given by following form

$$v_x(x, y, z) = v_x(x, y) \sin\left(\frac{\pi}{H} z\right), \quad (26)$$

$$v_y(x, y, z) = v_y(x, y) \sin\left(\frac{\pi}{H} z\right), \quad (27)$$

H is the thickness of the channel, integrating along the thickness, one obtains

$$q_x(x, y) = \int_0^H v_x(x, y, z) dz = \frac{2H}{\pi} v_x(x, y), \quad (28)$$

$$q_y(x, y) = \int_0^H v_y(x, y, z) dz = \frac{2H}{\pi} v_y(x, y), \quad (29)$$

substitute for v_x , v_y and change Φ_i^k to Φ_i in Eqs. (23) and (24), we can obtain following FEM equations with the variable of flow

$$A_{ij} \delta q_{x_j} + C_{ij} \delta q_{y_j} - D_{in} \delta P_n = X_i, \quad (30)$$

$$C_{ji} \delta q_{x_j} + B_{ij} \delta q_{y_j} - E_{in} \delta P_n = Y_i, \quad (31)$$

$$D_{jn} \delta q_{x_j} + E_{jn} \delta q_{y_j} = Z_n, \quad (32)$$

where X_i , Y_i and Z_n are the right-side item of Eqs. (23), (24) and (25), i and j indicate the number of velocity node, n is the number of pressure node, and

$$A_{ij} = \frac{\pi}{2H} \left(\int_{\Omega} 2\eta \frac{\partial \phi_j}{\partial x} \frac{\partial \Phi_i}{\partial x} d\Omega + \int_{\Omega} \eta \frac{\partial \phi_j}{\partial y} \frac{\partial \Phi_i}{\partial y} d\Omega + \int_{\Omega} \eta \frac{\partial \phi_j}{\partial z} \frac{\partial \Phi_i}{\partial z} d\Omega \right), \quad (33)$$

$$B_{ij} = \frac{\pi}{2H} \left(\int_{\Omega} \eta \frac{\partial \phi_j}{\partial x} \frac{\partial \Phi_i}{\partial x} d\Omega + \int_{\Omega} 2\eta \frac{\partial \phi_j}{\partial y} \frac{\partial \Phi_i}{\partial y} d\Omega + \int_{\Omega} \eta \frac{\partial \phi_j}{\partial z} \frac{\partial \Phi_i}{\partial z} d\Omega \right), \quad (34)$$

$$C_{ij} = \frac{\pi}{2H} \int_{\Omega} \eta \frac{\partial \phi_j}{\partial x} \frac{\partial \Phi_i}{\partial y} d\Omega, \quad (35)$$

$$D_{in} = \int_{\Omega} \phi_n \frac{\partial \Phi_i}{\partial x} d\Omega, \quad (36)$$

$$E_{in} = \int_{\Omega} \phi_n \frac{\partial \Phi_i}{\partial y} d\Omega, \quad (37)$$

The unknown variable of Eqs. (30), (31) and (32) is flow \mathbf{q} , because the flow is continuous at node, the global stiffness matrix equation for all the elements can be assembled after the elemental calculation.

By the finite piece method, we only divide element with thickness in the X - Y plane and need not to divide along direction Z , so the elements are much fewer than by 3D FEM, and the pre-processing become very simple.

The extra-stress tensor in X_i , Y_i and Z_n of Eqs. (30) and (31) is calculated by integrating along path line according to the constitutive equation. For steady flows, the particle acceleration can be expressed by the velocity [21]

$$\frac{D\mathbf{V}}{Dt} = \mathbf{V} \cdot \nabla \mathbf{V}, \quad (38)$$

making use of the above expression, the following particle tracking scheme is proposed

$$x'_i = x_i - v_i ds + \frac{ds^2}{2} \times \left(v_j \frac{\partial v_i}{\partial x_j} \right)^0 + \frac{ds^2}{6} \times \left[\left(v_j \frac{\partial v_i}{\partial x_j} \right)^1 - \left(v_j \frac{\partial v_i}{\partial x_j} \right)^1 \right] + O(ds)^4, \quad (39)$$

where x'_i is the particle coordinate at time t' and x_i is the coordinate at time $t' + ds$, the superscript 0 indicates the location at x_i , while the superscript 1 indicates the location at x_i^1 which is given by

$$x_i^1 = x_i - v_i ds + \frac{ds^2}{2} \times \left(v_j \frac{\partial v_i}{\partial x_j} \right)_0, \quad (40)$$

Eqs. (39) and (40) give particle location as a function of the residence time, which is essential for the calculation of the deformation tensor \mathbf{F} as a function of the residence time. The following relations are given

$$\frac{D\mathbf{F}_t(s)}{Ds} = \mathbf{L}(s)\mathbf{F}_t(s), \quad (41)$$

$$\mathbf{F}_t(s)_{s=0} = \mathbf{I}, \quad (42)$$

$$\mathbf{C}_t^{-1}(s) = \mathbf{F}_t(s)^{-1}[\mathbf{F}_t(s)^T]^{-1}, \quad (43)$$

where $s = t - t'$ is the residence time of the particle, $\mathbf{L}(s)$ is the velocity gradient, $\mathbf{F}_t(s)$ is the deformation tensor relative to the present configuration, $\mathbf{C}_t^{-1}(s)$ is the Finger strain tensor, \mathbf{I} is the unit tensor. The predictor-corrector formula is chosen for calculating deformation tensor

$$\mathbf{F}_t(t') = \mathbf{I} - \frac{ds}{2}(\mathbf{L} + \mathbf{L}' - ds\mathbf{L}\mathbf{L}') + O(ds^3), \quad (44)$$

where $ds = t - t'$, \mathbf{L} is the velocity gradient at location x_i , \mathbf{L}' is the velocity gradient at location x'_i . This equation gives only the “local” relative deformation tensor concerning two endpoints on the current increment ds , the following chain rule is repeatedly used to connect all the “local” to obtain the desired global deformation tensor

$$\mathbf{F}_t(t_3) = \mathbf{F}_t(t_3)\mathbf{F}_t(t_2), \quad (45)$$

Then the Cauchy-Green tensor and the Finger strain tensor can easily be calculated from the tensor \mathbf{F} according to their definition.

4. EXAMPLE AND DISCUSSION

To understand its solution accuracy and convergence rate of iteration we first analyze flow of the polymer melt in the rectangular cross-section channel and compare the results with three-dimensional finite element method.

The geometry and the coordinate system of the flow region are shown in Fig. 3. The main geometric parameters are given respectively as follow. The width of flow channel $W = 0.096\text{m}$, length $L = 4W$, the flow is calculated in channels with different aspect ratio H/W . H is thickness. The flow region is divided into 3D elements by using mapping mesh generation technology. The number of element divisions along thickness is 4 and along width is 8.

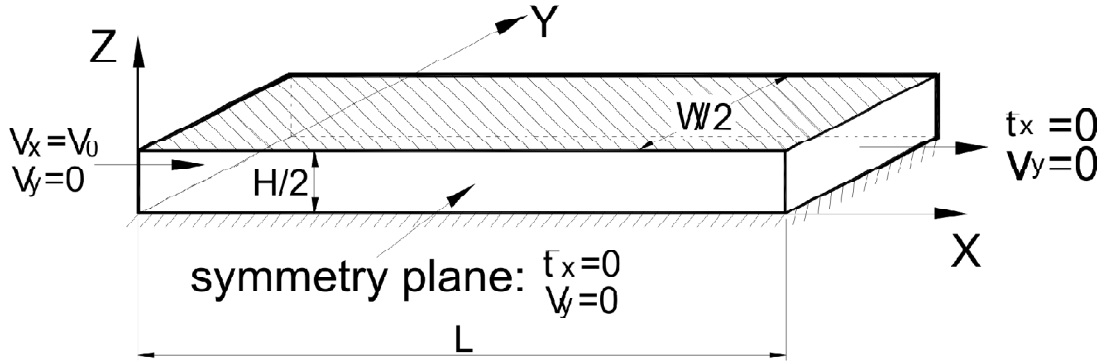


Figure 3: Schematic Diagram of the Rectangular Cross-section Channel Geometry and Boundary Conditions

To compare the results, the mesh of the finite piece method is the same as mesh of 3D FEM in X-Y plane. Melt is Low Density Polyethylene which relaxation spectrum used in this work are summarized in Tab. 1. θ is set to zero in this work. $\alpha = 12.47$, $\beta = 0.06$, $\eta_0 = 2365 P_a \cdot s$. Because convergence is difficult at high flow rates in the numerical simulation of K-BKZ model, we only analyze the flow at low rate.

Table 1
Linear Viscoelastic Spectrum for the Polymer Melt at 190°C [18]

k	$\lambda_k(s)$	$a_k(Pa)$
1	4.28×10^{-5}	$2.17 \times 10^{+5}$
2	2.07×10^{-4}	$9.18 \times 10^{+4}$
3	1.34×10^{-3}	$5.75 \times 10^{+4}$
4	9.02×10^{-3}	$2.43 \times 10^{+4}$
5	5.69×10^{-2}	$8.91 \times 10^{+3}$
6	3.53×10^{-1}	$2.34 \times 10^{+3}$
7	1.82×10^0	$3.21 \times 10^{+2}$
8	9.94×10^0	$1.24 \times 10^{+1}$

Boundary conditions are imposed according to the flow characteristics in the channel. As shown in Fig. 3, average velocity for the required flow rate is imposed at the entry section. As for fully developed flow at the exit section, velocity components perpendicular to the die axis X and the traction force along the axis X are specified to be zero, where \bar{t} is surface force. Non-slip condition is imposed on the stationary solid wall along with the symmetry condition imposed on the plane of symmetry XZ.

The predicted flow distributions q_x/q_0 for this channel at average velocity $V_0 = 0.01 m/s$ of the entry are compared with 3D FEM in Tab. 2, 3, Fig. 4 and 5. Where q_x is flow rate of unit width, q_0 is average flow rate. Tab. 2, 3 is the flow distributions in the lateral scan on exit and $X = 1/2L$ for varying H/W , the Fig. 4 shows the flow distributions in the lateral scan on exit, it is visible that the initially flat velocity profile becomes parabolic in the exit section. Fig. 5 shows the flow distributions on the longitudinal plane of symmetry. By comparison, we find that both the trend and the quantitative agreement are very good. And the agreement between the finite piece method and 3D FEM data is seen to be quantitatively satisfactory for different aspect ratio H/W . It also shows that accuracy improves when the thickness increases. The results of the $H/W=1/8$ channel is more precise than those of the $H/W=1/2$ channel. In addition, by predicting flow at other flow rate, we find the agreement between the finite piece and 3D FEM data is satisfactory also.

The overall pressure drop for the die length considered in the computation is plotted versus volumetric rate Q in Fig. 6. The overall agreement between the finite piece method and 3D FEM is good. It is seen that the pressure drop levels off at the highest flow rates after an initial rapid increase. But by calculating we found that the convergence became difficult at high flow rates. However, the pressure drop prediction of the finite piece method on the whole is not as close to the 3D FEM as flow rate. As shown in Fig. 6, the agreements are very good

Table 2
Axial Flow Rate Predicted by the Finite Piece Method and 3D FEM in Exit Section for the Rectangular Cross-section Channel

2y/W	q_x / q_0					
	H/W=1/8		H/W=1/4		H/W=1/2	
	3D FEM	FPM	3D FEM	FPM	3D FEM	FPM
0.000	1.1086	1.1056	1.2044	1.1971	1.3691	1.3468
0.125	1.1068	1.1056	1.1978	1.1963	1.3518	1.3366
0.250	1.1062	1.1056	1.1956	1.1920	1.3216	1.3044
0.375	1.1049	1.1056	1.1831	1.1800	1.2601	1.2443
0.500	1.1041	1.1038	1.1544	1.1525	1.1592	1.1460
0.625	1.0950	1.0960	1.0876	1.0871	1.0025	0.9936
0.750	1.0500	1.0545	0.9378	0.9436	0.7697	0.7671
0.875	0.8655	0.8761	0.6379	0.6499	0.4507	0.4549
1.000	0.0000	0.0000	0.0000	0.0000	0.0000	0.0000

Table 3
Axial Flow Rate Predicted by the Finite Piece Method and 3D FEM in $x=1/2L$ Section for the Rectangular Cross-section Channel

2y/W	q_x / q_0					
	H/W=1/8		H/W=1/4		H/W=1/2	
	3D FEM	FPM	3D FEM	FPM	3D FEM	FPM
0.000	1.1073	1.1066	1.1991	1.1946	1.3546	1.3459
0.125	1.1072	1.1066	1.1991	1.1963	1.3443	1.3356
0.250	1.1071	1.1066	1.1936	1.1894	1.3117	1.3048
0.375	1.1068	1.1057	1.1805	1.1765	1.2518	1.2474
0.500	1.1050	1.1040	1.1513	1.1490	1.1553	1.1541
0.625	1.0964	1.0962	1.0871	1.0871	1.0077	1.0120
0.750	1.0566	1.0581	0.9469	0.9514	0.7874	0.7969
0.875	0.8675	0.8752	0.6421	0.6537	0.4644	0.4765
1.000	0.0000	0.0000	0.0000	0.0000	0.0000	0.0000

at low flow rates. The results of the finite piece method is slight larger than 3D FEM at high flow rates. The discrepancies may be attributed to possible inadequacy of the series to accurately predict distributions along the Z direction, because we only use the first item of Fourier series. We also found the number of iterations of the finite piece method change little compared with 3D FEM. It does not decrease the rate of convergence to predict distributions by Fourier series.

We also calculate the flows in expansion channel with variable thickness. The geometry and the coordinate system are shown in Fig. 7. The sheet mold with the fishtail shaped has similar channel. If the results are precise, the finite piece method can be used to predict the flow distributions in this kind of die. Flow channel width of entry and exit are respectively $W1 = 0.096m$, $W2 = 2W1$, length $L = 4W1$, thickness $H1 = 1/8W$, $H2 = 1/12W$. The numerical results of axial velocity distributions are shown. Fig. 8 shows the flow distributions in the lateral scan on exit, Fig. 9 shows the flow distributions on the longitudinal plane of symmetry. It is obvious that the profile gets flatter than in the rectangular cross-section channel. Fig. 10 shows the pressure distributions on the longitudinal plane of symmetry. There is an abrupt variation in the trend of pressure distribution near the contraction mouth. It can be found that the results agree well with the results of 3D FEM. So it is proved that the variable width and thickness do not influence precision of the finite piece method as long as the thickness of channel is much thinner than width.

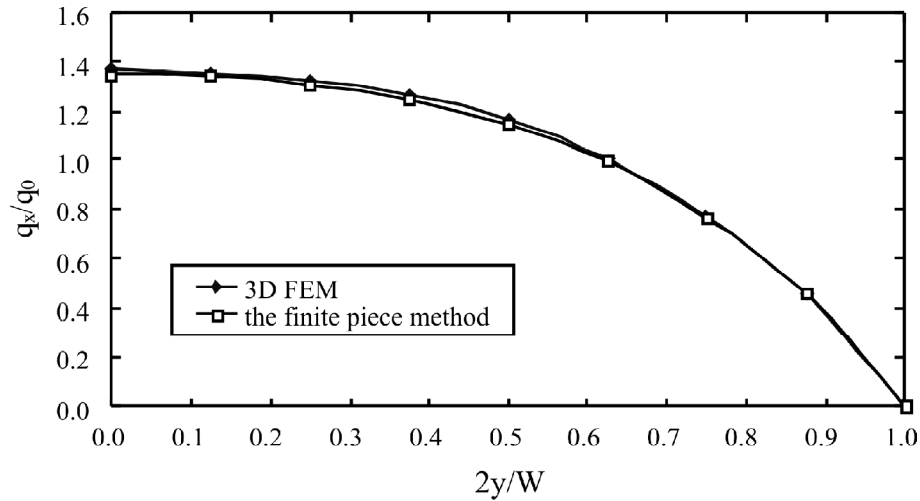


Figure 4: Axial Flow Rate Profile Predicted by the Finite Piece Method and 3D FEM in Exit Section for the Rectangular Cross-section Channel ($H/W=1/2$)

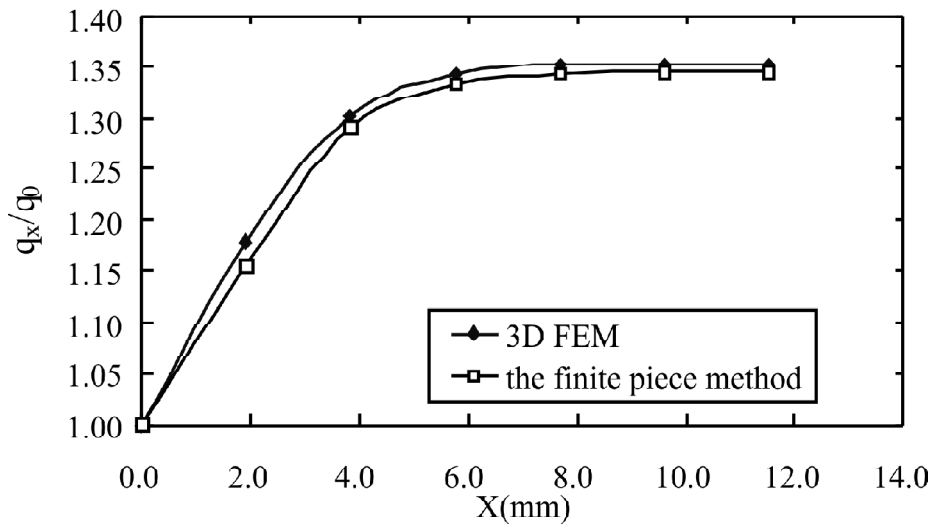


Figure 5: Axial Flow Rate Profile Predicted by the Finite Piece Method and 3D FEM in the X-Z Plane of Symmetry for the Rectangular Cross-section Channel ($H/W=1/2$)

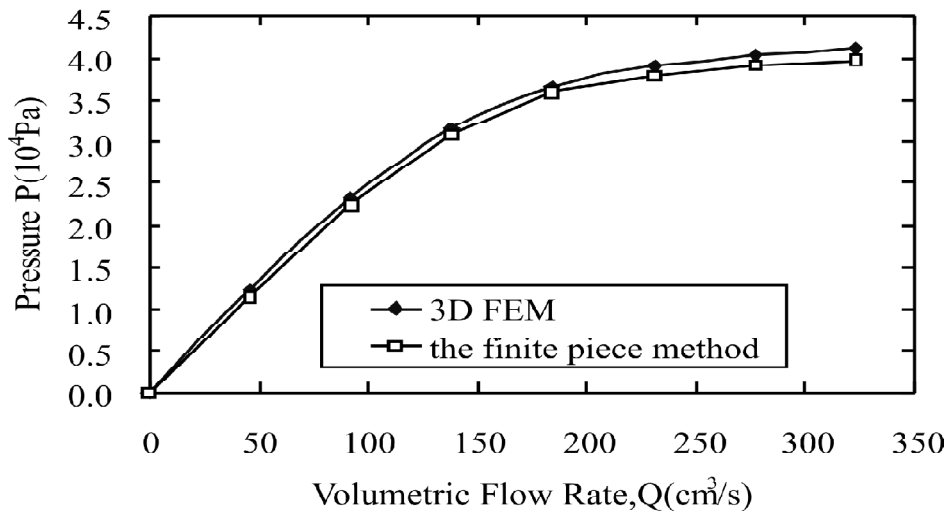


Figure 6: Prediction of the Pressure Drop for the Rectangular Cross-section Channel as a Function of Flow Rate ($H/W=1/2$)

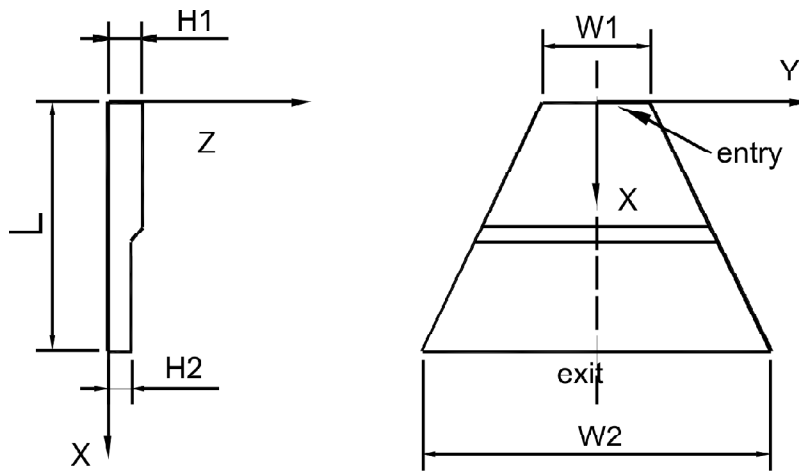


Figure 7: Schematic Diagram of the Expansion Channel Geometry and Coordinate System

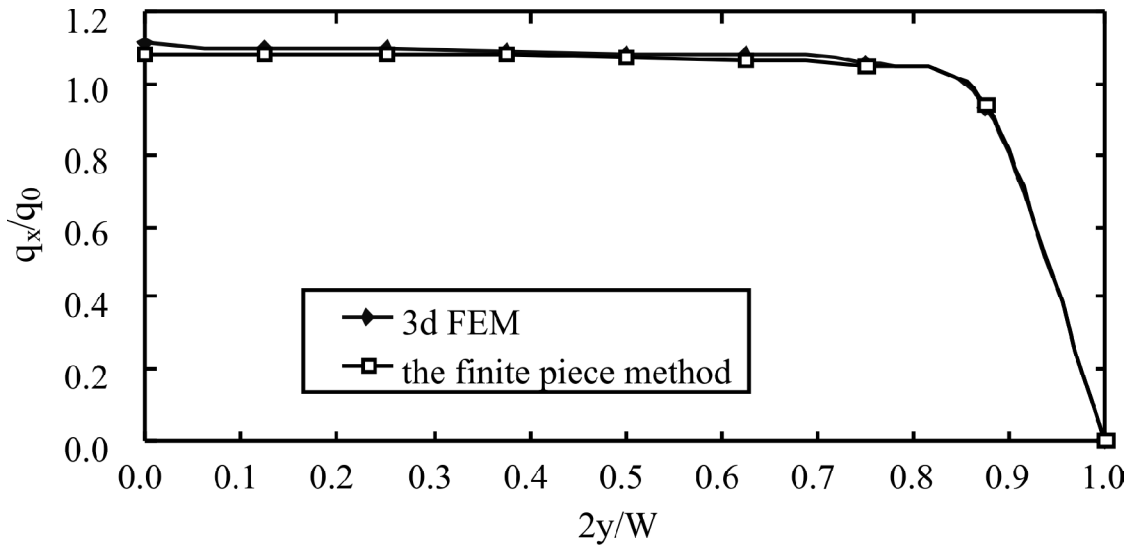


Figure 8: Axial Flow Rate Profile Predicted by the Finite Piece Method and 3D FEM in Exit Section for the Expansion Channel

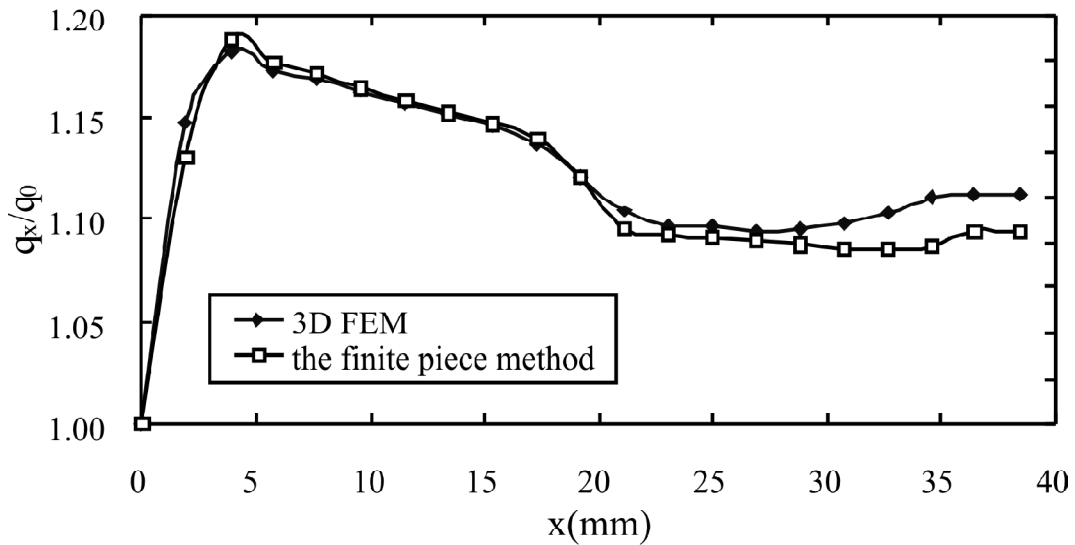


Figure 9: Axial Flow Rate Profile Predicted by the Finite Piece Method and 3D FEM in the X-Z Plane of Symmetry for the Expansion Channel

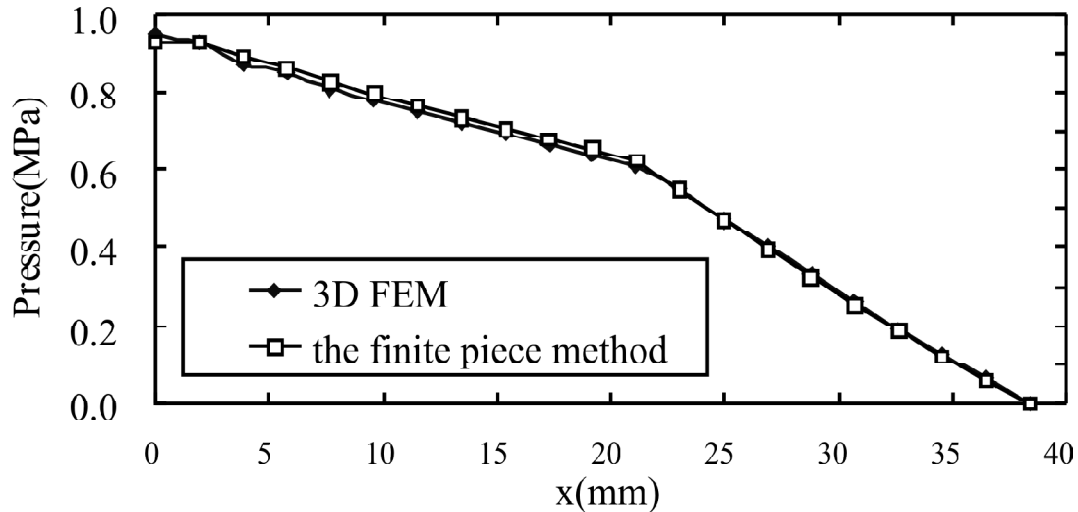


Figure 10: Pressure Predicted by the Finite Piece Method and 3D FEM in the X-Z Plane of Symmetry for the Expansion Channel

5. CONCLUSIONS

We have calculated the planar slit flow of viscoelastic fluid obeying K-BKZ model using the finite piece method. For three dimension planar flow, according to this method, we describe velocity using the approximating polynomial in X-Y plane and using Fourier series in Z direction. We just need to divide element with thickness in X-Y plane, so three dimensional finite element equation can be simplified to a two dimensional ones. It is found that the present method is relatively inexpensive and owing to the little demand on computational memory, the method can be used to solve large-scale three dimension problems.

The new method has been tested in planar channel with constant thickness and variable thickness. The comparison between the finite piece method and 3D FEM results is conducted. The distributions of velocity and pressure obtained by this method are very close to the 3D FEM results. The present results show that it is now possible to study complex flows using K-BKZ integral-type constitutive equations by this method. The reason of some discrepancies of pressure at high flow rate is that we only use the first item of Fourier series to approach the velocity in Z direction.

One of further work is needed to overcome the convergence difficulties at high flow rates in the numerical simulation of K-BKZ model. In addition, I think that not only planar slit but also space slit flow can be solved by the finite piece method, so further work is needed to give the way to solve space problem by this. Furthermore we can combine the finite piece method with 3D FEM to simulate the flow in the complex three dimension channel.

References

- [1] G. Mompean and M. Deville, "Corrigendum to Unsteady Finite Volume Simulation of Oldroyd-B fluid through a three-dimensional Planar Contraction," *J. Non-Newtonian Fluid Mech.*, **103**, 271–272, (2002).
- [2] S. C. Xue, N. Phan-Thien and R. I. Tanner, "Numerical Investigations of Lagrangian Unsteady Extensional Flows of Viscoelastic Fluids in 3-D Rectangular Ducts with Sudden Contraction," *Rheol. acta*, **37**, 158–169, (1998).
- [3] S. C. Xue, N. Phan-Thien and R. I. Tanner, "Three-dimensional Numerical Simulation of Viscoelastic Flows through Planar Contractions," *J. Non-Newtonian Fluid Mech.*, **74**, 195–245, (1998).
- [4] J. F. M. Schoonen, F. H. M. Swartjes, G. W. M. Peters, F. P. T., "Baaijens and H. E. H. Meijer, A 3D Numerical/experimental Study on a Stagnation Flow of a Polyisobutylene Solution," *J. Non-Newtonian Fluid Mech.*, **79**, 529–561, (1998).
- [5] S. Kihara, T. Gouda, K. Matsunaga and K. Funatsu. "Numerical Simulation of Three-dimensional Viscoelastic Flow within Dies," *Poly. Eng. Sci.*, **39**, 152–163, (1999).
- [6] Yue Mu, Guoqun Zhao, Chengrui Zhang, Anbiao Chen and Huiping Li, "Three-dimensional Simulation of Planar Contraction Viscoelastic Flow by Penalty Finite Element Method," *Int. J. Numer. Meth. Fluids*, **63**, 811–827, (2010).
- [7] Tanner R I., "From A to (KB)Z in Constitutive Relations," *J. Rheol.*, **32**, 673-702, (1988).

- [8] Akihiro Nishioka, Tatsuhiro Takahashi, Yuichi Masubuchi, Jun-ichi Takimoto, Kiyohito Koyama, "Description of Uniaxial, Biaxial, and Planar Elongational Viscosities of Polystyrene Melt by the K-BKZ Model," *J. Non-Newtonian Fluid Mech.*, 287-301, (2000).
- [9] X. L. Luo, E. Mitsoulis, "A Numerical Study of the Effect of Elongational Viscosity on Vortex Growth in Contraction Flows of Polyethylene Melts," *Journal of Rheology*, **34**, 309–342, (1990).
- [10] B. Bernstein, K. A. Feigl, E. T. Olsen, "Steady Flows of Viscoelastic Fluids in Axisymmetric Abrupt Contraction Geometry: Acomparison of Numerical Results," *J. Rheol.* **3**, 53–71, (1994).
- [11] J. Sun, N. Phan-Thien, R. I. Tanner, "Extrudate Swell through an Orifice Die," *Rheol. Acta*, **35**, 1–12, (1996).
- [12] X. L. Luo, R. I. Tanner, "Finite Element Simulation of Long and Short Circular Die extrusion Experiments using Integral Models," *Comput. Methods Appl. Mech. Eng.*, **25**, 9–22, (1988).
- [13] G. Barakos, E. Mitsoulis, "Aconvergence Study for the Numerical Simulation of the IUPAC-LDPE Extrusion Experiments," *J. Non-Newtonian Fluid Mech.*, **58**, 315-329, (1995).
- [14] A. Bach, H. K. Rasmussen, P. Y. Longin, O. Hassager, "Growth of Non-axisymmetric Disturbances of the Free Surface in the Filament Stretching Rheometer: Experiments and Simulation," *J. Non-Newtonian Fluid Mech.*, **108**, 163–186, (2002).
- [15] T. Eriksson, H. K. Rasmussen, "The Effects of Polymer Melt Rheology on the Replication of Surface Microstructures in Isothermal Moulding," *J. Non-Newtonian Fluid Mech.*, **127**, 91–200, (2005).
- [16] H. K. Rasmussen, K. Yu, "On the Burst of Branched Polymer Melts during Inflation," *Rheol. Acta*, **47**, 149–157, (2008).
- [17] H. K. Rasmussen, T. Eriksson, "Gas Displacement of Polymer Melts in a Cylinder: Experiments and Viscoelastic Simulations," *J. Non-Newtonian Fluid Mech.*, **143**, 1–9, (2007).
- [18] Yves Beraux, Jean-Robert Clermont, "Numerical Simulation of Complex Flows of Non-Newtonian Fluids using the Stream Tube Method and Memory Integral Constitutive Equations," *J. Non-Newtonian Fluid Mech.*, **21**, 371-389, (1995).
- [19] Cheung Y. K. and Kong J., "The Application of a New Finite Strip to the Free Vibration of Rectangular Plates of Varying Complexity," *J. Sound Vibration*, **23**, 341-353, (1995).
- [20] Evan Mitsoulis, "Numerical Simulation of Confined Flow of Polyethylene Melts Around a Cylinder in a Planar Channel," *J. Non-Newtonian Fluid Mech.*, **76**, 327–350, (1998).
- [21] Luo X. L., Tanner R. I., "A Streamline Element Scheme for Solving Viscoelastic Flow Problems Part II Integral Constitutive Models," *J. Non-Newtonian Fluid Mech.*, **22**, 61-89, (1986).